Deletion of the *Slo3* gene abolishes alkalization-activated K^+ current in mouse spermatozoa

Xu-Hui Zeng, Chengtao Yang, Sung Tae Kim, Christopher J. Lingle[1], and Xiao-Ming Xia

Department of Anesthesiology, Washington University School of Medicine, St. Louis, MO 63110

Edited* by David E. Clapham, Children's Hospital Boston, Boston, MA, and approved February 28, 2011 (received for review January 5, 2011)

Mouse spermatozoa express a pH-dependent K^+ current (KSper) thought to be composed of subunits encoded by the *Slo3* gene. However, the equivalence of KSper and *Slo3*-dependent current remains uncertain, because heterologous expression of *Slo3* results in currents that are less effectively activated by alkalization than are native KSper currents. Here, we show that genetic deletion of *Slo3* abolishes all pH-dependent K^+ current at physiological membrane potentials in corpus epididymal sperm. A residual pH-dependent outward current (I_{Kres}) is observed in $Slo3^{-/-}$ sperm at potentials of >0 mV. Differential inhibition of KSper/Slo3 and I_{Kres} by clofilium reveals that the amplitude of I_{Kres} is similar in both wild-type (wt) and $Slo3^{-/-}$ sperm. The properties of I_{Kres} suggest that it likely represents outward monovalent cation flux through CatSper channels. Thus, KSper/Slo3 may account for essentially all mouse sperm K^+ current and is the sole pH-dependent K^+ conductance in these sperm. With physiological ionic gradients, alkalization depolarizes $Slo3^{-/-}$ spermatozoa, presumably from CatSper activation, in contrast to Slo3/KSper-mediated hyperpolarization in wt sperm. $Slo3^{-/-}$ male mice are infertile, but $Slo3^{-/-}$ sperm exhibit some fertility within in vitro fertilization assays. $Slo3^{-/-}$ sperm exhibit a higher incidence of morphological abnormalities accentuated by hypotonic challenge and also exhibit deficits in motility in the absence of bicarbonate, revealing a role of KSper under unstimulated conditions. Together, these results show that KSper/Slo3 is the primary spermatozoan K^+ current, that KSper may play a critical role in acquisition of normal morphology and sperm motility when faced with hyperosmotic challenges, and that Slo3 is critical for fertility.

Definition of the molecular identities and physiological roles of K^+ channels in mammalian sperm is expected to provide key insights into regulation of sperm motility and activation. An alkalization-activated K^+ conductance, termed KSper, appears to be the primary K^+ conductance in mouse spermatozoa (1). It has been proposed that hyperpolarization resulting from alkalization-induced KSper activation will work in concert with the simultaneous activation of the pH-sensitive Ca^{2+}-selective CatSper channel to promote Ca^{2+} influx essential for the initiation of hyperactivation (1, 2). Thus, KSper activation is proposed to play a critical role in the complex set of physiological and biochemical changes, collectively termed "capacitation" (3–5), that are essential for the ability of sperm to produce fertilization.

Recently, it has been shown that genetic knockout (KO) of a likely molecular component of KSper (6), the testis-specific, pH-sensitive Slo3 K^+ channel (7), results in infertile males and, in testicular sperm, abolishes activation of a K^+ current by NH_4Cl, which is thought to act via cytosolic alkalization. However, the magnitude of K^+ current and pH-dependent K^+ current in testicular sperm is modest compared with that in epididymal sperm, and it remains unclear to what extent Slo3 may account for K^+ conductance in the more mature epididymal sperm. Another unresolved issue is that the pH and voltage dependence of KSper current described in spermatozoa (1) differs in important ways from the properties of Slo3 currents studied with heterologous expression in oocytes (8, 9). In particular, whereas appreciable activation of KSper occurs between pH 6.5 and 7.0 at physiological potentials, Slo3 channels exhibit almost no activation at pH 7.0, even at potentials up to +100 mV.

Previous work on native KSper therefore leaves several unresolved questions. First, does Slo3 completely account for KSper? Second, is KSper the sole pH-activated K^+ conductance in mouse sperm? Third, are there other sperm K^+ conductances at physiological potentials? Finally, does KSper play any functional role in sperm independent of that associated with cytosolic alkalization? Here we report the generation of a unique mouse strain with a mutated *Slo3* gene and specifically examine the consequences of *Slo3* deletion on whole-cell current and voltage behavior of spermatozoa from corpus epididymis. Our results indicate that *Slo3* accounts for virtually all spermatozoan K^+ current and alkalization-dependent K^+ current at potentials negative to 0 mV. Although *Slo3* deletion abolishes fertility, it only partially disrupts in vitro fertilization (IVF). We propose that deficits in sperm motility and osmoregulation that precede alkalization may be the principal factors contributing to loss of fertility.

Results

***Slo3* Deletion Abolishes Most, but Not All, Alkalization-Activated Current.** A description of the *mSlo3* KO construct is provided in Fig. S1*A*. We designed the targeted allele to generate a Slo3–eGFP-tagged knock-in animal, in which enhanced GFP (eGFP) was fused in-frame with exon 27, with the aim of allowing visualization of Slo3 protein. Subsequently, exon 27, along with eGFP, was deleted by breeding with Cre-deleter mice to generate $Slo3^{-/-}$ mice. We confirmed that the Slo3–eGFP construct generated normal currents in oocytes. Furthermore, injection into oocytes of cRNA corresponding to Slo3 with exon 27 deleted produced no detectable current or channel openings (Fig. S2). In testis from $Slo3^{-/-}$ KO animals, expression of mRNA arising from the mutated gene was reduced to ~20% in comparison with wild-type (wt) *Slo3* message levels (Fig. S1*D*). Importantly, no residual truncated Slo3 protein was detected from $Slo3^{-/-}$ testes (Fig. S1 *E–G*). Quantitative RT-PCR confirmed that expression of *Slo3* message is specific to the testis (Fig. S3).

Whole-cell recordings from the cytoplasmic droplet of wt mouse spermatozoa revealed a pronounced K^+ conductance (Fig. 1*A*), consistent with the described KSper current (1). Our extracellular saline contained 2 mM Ca^{2+} to reduce endogenous CatSper current (10). Spermatozoa from $Slo3^{-/-}$ mice exhibited a markedly reduced K^+ conductance (Fig. 1 *A* and *B*). With a pipette saline of pH 8.0, the average outward current flux at +100 mV was 413 ± 13 pA (n = 25) in wt spermatozoa; 209 ± 20 pA (n = 10) from $Slo3^{+/-}$ spermatozoa; and 85 ± 11 pA (n = 13) in $Slo3^{-/-}$ spermatozoa (Fig. 1*B*). Given the documented

Author contributions: X.-H.Z., C.Y., C.J.L., and X.-M.X. designed research; X.-H.Z., C.Y., S.T.K., C.J.L., and X.-M.X. performed research; X.-M.X. contributed new reagents/analytic tools; X.-H.Z., C.Y., and X.-M.X. analyzed data; and C.Y. and C.J.L. wrote the paper.

The authors declare no conflict of interest.

*This Direct Submission article had a prearranged editor.

[1]To whom correspondence should be addressed. E-mail: clingle@morpheus.wustl.edu.

This article contains supporting information online at www.pnas.org/lookup/suppl/doi:10.1073/pnas.1100240108/-/DCSupplemental.

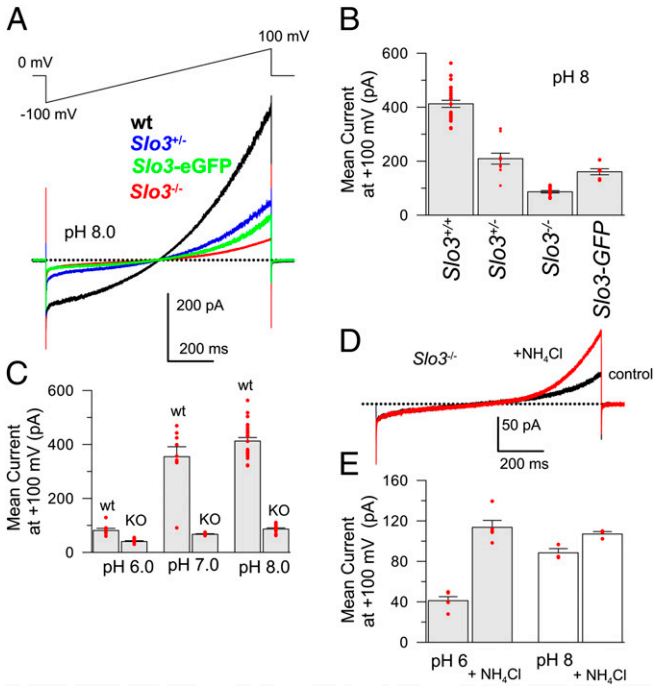

Fig. 1. KO of *Slo3* results in removal of most K^+ current in corpus epididymal sperm. (*A*) A 1-s voltage ramp was used to activate current from wt, *Slo3*$^{-/-}$ (red), *Slo3*$^{+/-}$ (blue), and *Slo3*–eGFP$^{+/+}$ (green) spermatozoa. Each example approximates the average behavior for that particular genotype. Pipette pH was 8.0; intracellular and extracellular salines each contained 160 mM K·Mes, with 2 mM extracellular Ca^{2+} to reduce monovalent flux through CatSper channels. (*B*) Mean current estimates at +100 mV with a cytosolic pH of 8.0 are plotted for four genotypes (wt: n = 25 cells, 17 mice; *Slo3*$^{+/-}$: 10 cells, 4 mice; *Slo3*$^{-/-}$: 13 cells, 8 mice; *Slo3–eGFP*: 6 cells, 4 mice). (*C*) Mean current measured at +100 mV is plotted for wt and *Slo3*$^{-/-}$ sperm at pH 6.0 (wt: n = 8, 2 mice; KO: n = 10, 4 mice), 7.0 (wt: 9 cells, 2 mice; KO: 6 cells, 2 mice), and 8.0 (wt: 25 cells, 17 mice; KO:13 cells, 8 mice). (*D*) Currents were activated in a *Slo3*$^{-/-}$ sperm with the ±100-mV voltage ramp with a pH 6.0 pipette solution. Current during application of 10 mM NH_4Cl is in red. (*E*) Mean current was measured at +100 mV in *Slo3*$^{-/-}$ sperm before and during application of NH_4Cl with a pipette solution at either pH 6.0 (n = 5, two mice) or pH 8.0 (n = 3, one mouse).

monovalent cation permeability of CatSper, some K^+ current at +100 mV, even with 2 mM Ca^{2+}_o, is likely to arise from native CatSper channels (11). Net K^+ current in *Slo3–eGFP*$^{+/+}$ sperm was also reduced to an extent similar to *Slo3*$^{+/-}$ sperm (Fig. 1 *A* and *B*). In wt sperm, increases in pipette pH increased total sperm K^+ current monitored at +100 mV (Fig. 1*C*). Alkalization also mildly increased outward current in *Slo3*$^{-/-}$ sperm (Fig. 1*C*), suggesting the presence of an additional alkalization-activated outward current. Consistent with this idea, application of 10 mM NH_4Cl to *Slo3*$^{-/-}$ sperm resulted in increases in outward current (Fig. 1*D*), but only at voltages positive to 0 mV (Fig. 1*D*). NH_4Cl increased current at +100 mV with pipette solutions weakly buffered to either pH 6.0 or 8.0 (Fig. 1*E*). Here, we term the voltage-activated and pH-sensitive outward current present in *Slo3*$^{-/-}$ sperm as I_{Kres}, in the absence of definition of its molecular basis. The absence of alkalization-activated current at potentials negative to 0 mV in *Slo3*$^{-/-}$ sperm indicates that KSper/Slo3 accounts for all alkalization activated K^+ current negative to 0 mV. A remaining question is why KSper/Slo3 in native sperm is robustly activated at potentials negative to 0 mV at pH 7.0, whereas heterologously expressed Slo3 exhibits no obvious activation under such conditions (Fig. S4; ref. 8).

Voltage Dependence and Kinetic Properties Distinguish I_{Kres} from Slo3/KSper. Currents in wt and *Slo3*$^{-/-}$ sperm were also compared by using standard voltage-step protocols with symmetrical K^+ [intracellular pH (pH_i) 8.0; Fig. 2 *A* and *C*]. wt sperm exhibited a larger resting K^+ conductance at negative potentials (Fig. 2 *A*, *B*, and *E*) than *Slo3*$^{-/-}$ sperm. Voltage steps elicited both instantaneous and time-dependent current activation in wt sperm (Fig. 2*B*), whereas *Slo3*$^{-/-}$ sperm exhibited exclusively time-dependent activation at potentials above approximately +50 mV (Fig. 2*D*). Net steady-state conductance in wt sperm increased linearly up to approximately +100 mV before saturating, whereas in *Slo3*$^{-/-}$ sperm the increase in conductance was only observed from approximately +50 up to +200 mV (Fig. 2*E*). Thus, I_{Kres}, at least in *Slo3*$^{-/-}$ sperm, contributed minimally to currents negative to 0 mV and exhibited a pronounced voltage-dependent activation distinct from the *Slo3*-dependent current. The total K^+ current (I_{Ktot}) in wt sperm presumably represents both KSper/Slo3 and I_{Kres}. Interestingly, at +200 mV, the net conductance between wt and *Slo3*$^{-/-}$ sperm differed by <20%. Therefore, if I_{Kres} is similar in density in both wt and *Slo3*$^{-/-}$ sperm, the component of conductance arising from KSper/Slo3 must exhibit a substantial net reduction between 0 and +200 mV. Another distinguishing feature between I_{Kres} in *Slo3*$^{-/-}$ sperm and the K^+ current in wt sperm is the larger current variance observed in wt sperm. This larger current variance in wt sperm is qualitatively consistent with the idea that the Slo3 channel mediates a relatively large single channel current (8, 9).

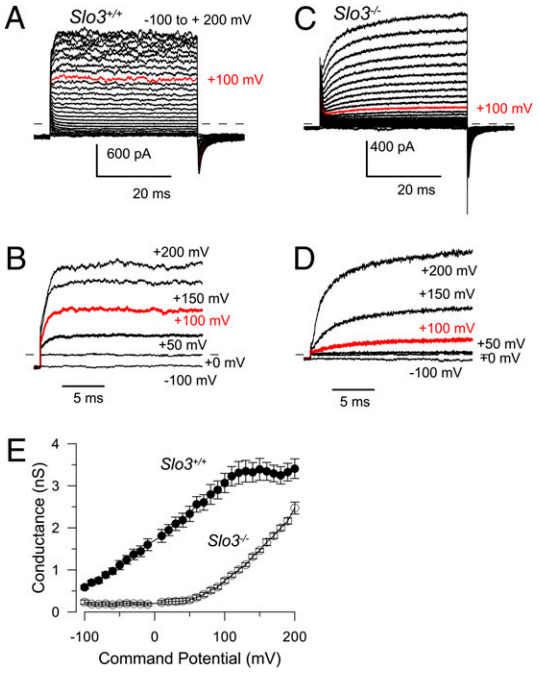

Fig. 2. Distinct voltage dependence and kinetic properties of current present following *Slo3* deletion. (*A*) Traces show current activated in a wt sperm from a holding potential of −100 mV with steps up to +200 mV. Red trace highlights current activated at +100 mV. (Pipette pH 8.0.) (*B*) Activation of current from traces in *A* after subtraction of uncompensated capacity currents (using the step to 0 mV for digital subtraction) reveals both instantaneous and time-dependent current activation. (*C*) Traces show currents from a *Slo3*$^{-/-}$ sperm. (Pipette pH 8.0.) (*D*) After subtraction of uncompensated capacity transients, currents in *Slo3*$^{-/-}$ sperm are only activated at potentials positive to 0 mV and exhibit prominent voltage-dependent increases in current activation. (*E*) Steady-state currents for wt (n = 11) and *Slo3*$^{-/-}$ (n = 9) sperm were converted to conductances assuming a 0-mV reversal potential. At potentials negative to 0 mV, essentially all residual K^+ conductance is absent in *Slo3*$^{-/-}$ sperm.

Clofilium Distinguishes the Relative Contributions of Slo3/KSper and I_{Kres} in wt Sperm. Clofilium has been shown to irreversibly block KSper (1). Here, blockade by 50 μM clofilium reduced total K^+ current in wt sperm and abolished the high current variance behavior of the wt currents (Fig. 3*A*). Washout of clofilium (Fig. 3 *A* and *B*) in wt sperm resulted in both an initial more rapid component of recovery and then an essentially irreversible component of block (Fig. 3*B*). In contrast, block of I_{Kres} in *Slo3*$^{-/-}$ sperm (Fig. 3*C*) was readily reversible (Fig. 3 *C* and *D*). We compared net conductance before, during, and ~3 min after washout from 50 μM clofilium for both wt (Fig. 3*E*) and *Slo3*$^{-/-}$ sperm (Fig. 3*F*). Whereas in *Slo3*$^{-/-}$ sperm I_{Kres} completely recovered from block, in wt sperm, blockade of most of the K^+ current persisted. Thus, the unblocked current after brief washout of clofilium in wt sperm represents endogenous I_{Kres}. Comparison of the net K^+ conductance after washout of clofilium showed that I_{Kres} was essentially identical in both wt and *Slo3*$^{-/-}$ sperm. The difference between the total K^+ conductance in a given sperm and the component attributable to I_{Kres} (the current persisting after washout of clofilium) essentially isolates KSper, the component of current attributable to Slo3. For wt sperm, the Slo3-dependent conductance increased up through +100 mV and then exhibited substantial block at more positive potentials (Fig. 3*G*). The apparent voltage-dependent block of conductance of the Slo3-component of current seemed unusual given published descriptions of heterologously expressed Slo3 (8, 9). However, the composition of the pipette solutions used for sperm recordings included cations, such as Mg^+ and Na^+, that are not typically used during study of heterologously expressed Slo3. We therefore tested the sperm cytosolic solution on heterologously expressed Slo3 channels and confirmed that both Mg^{2+} and Na^+ probably contribute to the flattening and block of conductance observed for KSper in native sperm (Fig. 3*G* and Fig. S5).

Quinine reversibly inhibits KSper (1), and its stereoisomer, quinidine, blocks heterologously expressed Slo3 (12). Here, we found that quinidine inhibition of total sperm K^+ current (Fig. S6 *A* and *B*) was comparable to that of heterologously expressed Slo3 (12). However, quinidine, which also inhibits a variety of other channels (13–15), was ineffective in distinguishing between inhibition of total K^+ current and I_{Kres} (Fig. S6 *C–E*).

Slo3/KSper Current Is Essential for Alkalization-Activated Hyperpolarization in Spermatozoa. The current–clamp behavior of wt and *Slo3*$^{-/-}$ sperm was compared in physiological Na_o/K_i solutions. In wt sperm with a pipette solution of pH 6.0, extracellular application of 10 mM NH_4Cl resulted in a pronounced hyperpolarization (Fig. 4*A*), whereas in *Slo3*$^{-/-}$ sperm, application of 10 mM NH_4Cl slightly depolarized the sperm membrane potential (Fig. 4*B*). The average resting potential of wt sperm was −13.1 ± 2.1 mV at pH_i 6 (n = 5) and −44.2 ± 1.4 mV at pH_i 8 (n = 5; Fig. 4 *C* and *D*). For *Slo3*$^{+/-}$ sperm, the membrane potential was −13.3 ± 1.9 mV (n = 5) at pH_i 6 and −41.4 ± 2.4 mV (n = 5) at pH_i 8. In contrast, for *Slo3*$^{-/-}$ sperm, the resting potential was −7.2 ± 1.4 mV (n = 8) at pH_i 6 compared with −2.4 ± 1.2 mV (n = 7) at pH_i 8. Thus, deletion of *Slo3* resulted in an abolition of the ability of cytosolic alkalization to produce hyperpolarization.

***Slo3*$^{-/-}$ Male Mice Are Infertile, but Capacitated *Slo3*$^{-/-}$ Sperm Exhibit Partial IVF Success.** *Slo3*$^{-/-}$ male mice were unable to fertilize wt females, despite the presence of fertilization plugs (Fig. S7*A*). Litter sizes resulting from *Slo3*–GFP and *Slo3*$^{+/-}$ males were indistinguishable from wt (Fig. S7*B*). In a separate test, *Slo3*$^{-/-}$ males failed to result in fertilized ova following mating with superovulated females (Fig. S7 *C* and *D*). We also examined the ability of sperm to produce fertilization of isolated wt oocytes with intact zona pellucida (ZP). Oocytes harvested from superovulating wt females were incubated with capacitated sperm from wt, *Slo3*$^{+/-}$, or *Slo3*$^{-/-}$ mice. From six trials, we observed that ~35.1% (94/268) of oocytes were successfully fertilized by wt sperm. *Slo3*$^{-/-}$ sperm resulted in fertilization of ~10.9% (41/376) of the oocytes, whereas *Slo3*$^{+/-}$ sperm resulted in 39% (74/215)

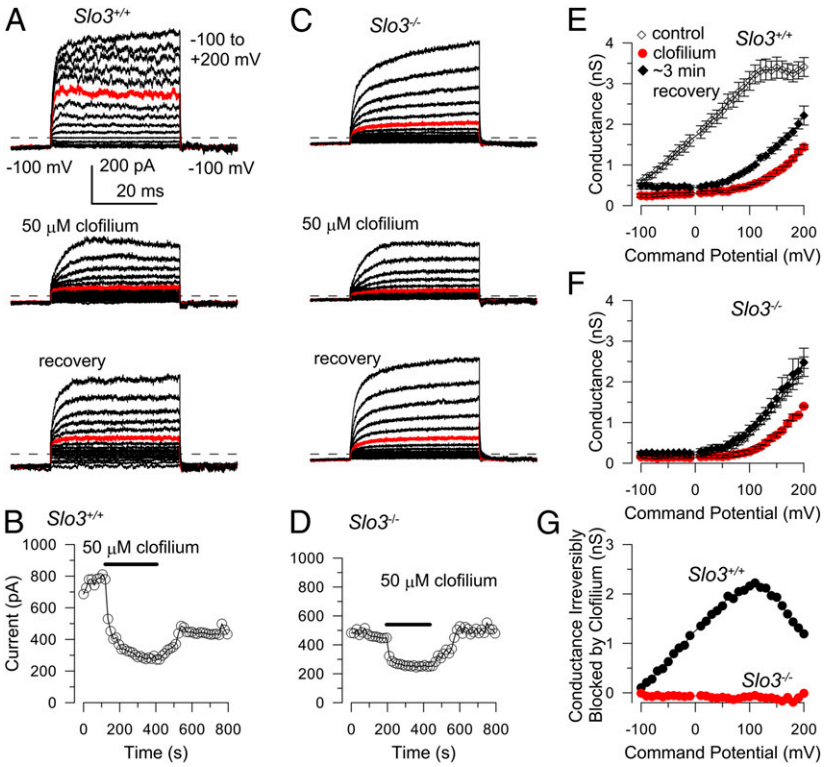

Fig. 3. Clofilium distinguishes between I_{KSper} and I_{Kres}, revealing that I_{Kres} is identical in both wt and *Slo3*$^{-/-}$ sperm. (*A*) Top traces show currents activated in a wt sperm with cytosolic pH 8.0 with voltage steps up to +200 mV (red, +100 mV). Capacity transients were digitally subtracted. Application of 50 μM clofilium (middle traces) blocks most rapidly activating current and most current at +100 mV. Most current at +100 mV remains inhibited following washout of clofilium (bottom traces). (*B*) The time course of onset and recovery from block of wt currents by 50 μM clofilium (at +200 mV) is plotted. Washout from clofilium shows both rapid and essentially irreversible components of recovery. (*C*) Clofilium inhibits outward current in *Slo3*$^{-/-}$ sperm, but clofilium inhibition is quickly reversed upon washout. (*D*) Time course of clofilium block and recovery in *Slo3*$^{-/-}$ sperm. (*E*) Average net conductance from wt sperm before (open circles), during block by 50 μM clofilium (red circles), and after ~180 s washout of clofilium (diamonds). (n = 5 cells.) (*F*) Average net conductance from *Slo3*$^{-/-}$ sperm for control (open circles), 50 μM clofilium (red circles), and after wash (diamonds). (n = 4 cells.) (*G*) The component of net conductance irreversibly blocked by clofilium for wt and *Slo3*$^{-/-}$ sperm is plotted.

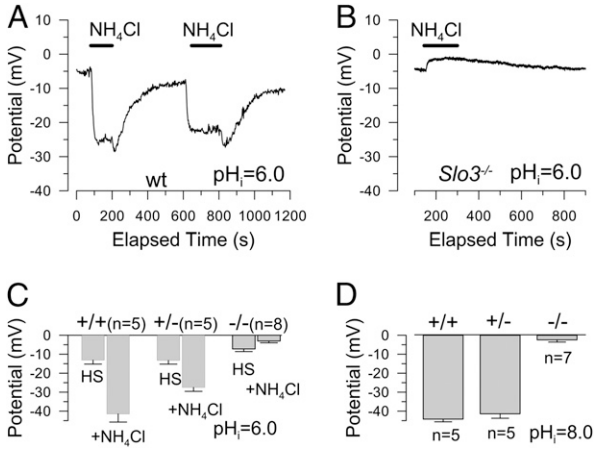

Fig. 4. Spermatozoa from *Slo3*$^{-/-}$ mice lack alkalization-mediated hyperpolarization. (*A*) Membrane potential was recorded in a wt mouse spermatozoan bathed in HS medium, and 10 mM NH_4Cl was applied as indicated. (Pipette saline pH 6.0.) (*B*) Membrane potential in a *Slo3*$^{-/-}$ spermatozoan was monitored, and NH_4Cl was applied as indicated. (*C*) Mean values for resting potential for either *Slo3*$^{+/+}$, *Slo3*$^{+/-}$, or *Slo3*$^{-/-}$ sperm are plotted for both HS and for HS supplemented with 10 mM NH_4Cl, all with pH 6.0 intracellular saline. (*D*) Mean values for membrane potential for *Slo3*$^{+/+}$, *Slo3*$^{+/-}$, and *Slo3*$^{-/-}$ sperm are plotted. (Pipette saline pH 8.0.)

fertilization. *Slo3*$^{-/-}$ sperm retained some competence to fertilize oocytes.

Caudal Epididymal Sperm from *Slo3*$^{-/-}$ Mice Exhibit Modest Deficits in Motility. The motility of caudal epididymal sperm from wt, *Slo3*$^{+/-}$, and *Slo3*$^{-/-}$ mice was examined by using computer-assisted sperm analysis (CASA) after swim-out into human tubal fluid (HTF) medium with 25 mM $NaHCO_3$. The overall fraction of motile sperm exhibited only minor differences over 90 min among wt, *Slo3*$^{+/-}$, and *Slo3*$^{-/-}$ sperm (Fig. S8*A*). However, over the 90-min period, the percentage of sperm exhibiting progressive motility gradually increased in wt, whereas *Slo3*$^{-/-}$ exhibited no change (Fig. S8*B*). Over 90 min, both *Slo3*$^{-/-}$ and *Slo3*$^{+/-}$ sperm exhibited lower average path velocities (Fig. S8*C*) and linear average linear velocities (Fig. S8*D*) than *Slo3*$^{+/+}$ sperm. Normalized distributions of the percentages of sperm exhibiting different path velocities (VAP; Fig. S8*E*) and linear velocities (VSL; Fig S8*F*) showed that, whereas at time = 0 the distributions of VAP and VSL were essentially identical for all three genotypes, at 90 min *Slo3*$^{-/-}$ sperm exhibited a pronounced increase in the fraction of sperm exhibiting slower velocities. No differences in sperm number were observed between wt and *Slo3*$^{-/-}$ animals.

Absence of Slo3 Interferes with Osmoregulation. Mammalian sperm fertility is dependent on the ability of sperm to maintain normal volume regulation after mixing with seminal fluid and entry into the vagina. Release from the epididymis involves movement from an environment of ~420 mmol/kg into one near 310 mmol/kg (16), resulting in appreciable osmotic stress. An inability to undergo appropriate volume regulation results in morphologically abnormal sperm epitomized by swelling (16, 17), angular flagella, and even hairpins (18), although such morphological abnormalities are also observed under swim-out into 310 mmol/kg solutions (19).

A morphological difference between wt and *Slo3*$^{-/-}$ sperm has been reported (6). We therefore designed an experiment to evaluate whether the absence of KSper/Slo3 might contribute to difficulties in osmotic regulation. Caudal epididymal sperm were allowed to swim up into an Hepes-buffered saline (HS)-430 medium. After dilution to final osmolalities of 430, 310, or 230 mmol/kg, either in the presence or absence of 25 mM $NaHCO_3$, sperm behavior was monitored at 0, 30, and 60 min. Approximately 100 motile sperm in each solution and time point were then categorized into one of three morphologies: straight, bent, or hairpin. For both wt and *Slo3*$^{-/-}$ sperm, morphology was sensitive to the osmolality of the medium. Solutions of lower osmolality (230 and 310 mmol/kg) resulted in a marked increase in bent and hairpin morphologies (Fig. 5*A*), compared with 430 mmol/kg. However, compared with wt, *Slo3*$^{-/-}$ sperm exhibited a significant increase in abnormal morphologies in both 230- and 310 mmol/kg solutions. There was no difference between wt and *Slo3*$^{-/-}$ in the percentage of hairpin/bent morphologies in HS-430–BC, consistent with the idea that maintenance in a 430-mmol/kg solution protects against deficits in volume regulation associated with the absence of Slo3. Differences in sperm morphology were also pronounced when wt and *Slo3*$^{-/-}$ sperm were compared in the absence of $NaHCO_3$ (Fig. 5*B*). Thus, wt and *Slo3*$^{-/-}$ sperm exhibited marked functional differences, even in the absence of any stimulatory factor that might elevate pH or cytosolic cAMP.

One might expect the differences in morphology between wt and *Slo3*$^{-/-}$ sperm to be reflected in motility differences. Inspection of videos of wt and *Slo3*$^{-/-}$ sperm with 310 mmol/kg solutions with 25 mM $NaHCO_3$ clearly showed active motility in both populations, consistent with the CASA results, with a notable occurrence of actively swimming sperm with hairpins (Movies S1 and S2). In contrast, after dilution into 310 mmol/kg solution in the absence of $NaHCO_3$, *Slo3*$^{-/-}$ sperm exhibited pronounced motility deficits with little progressive motion

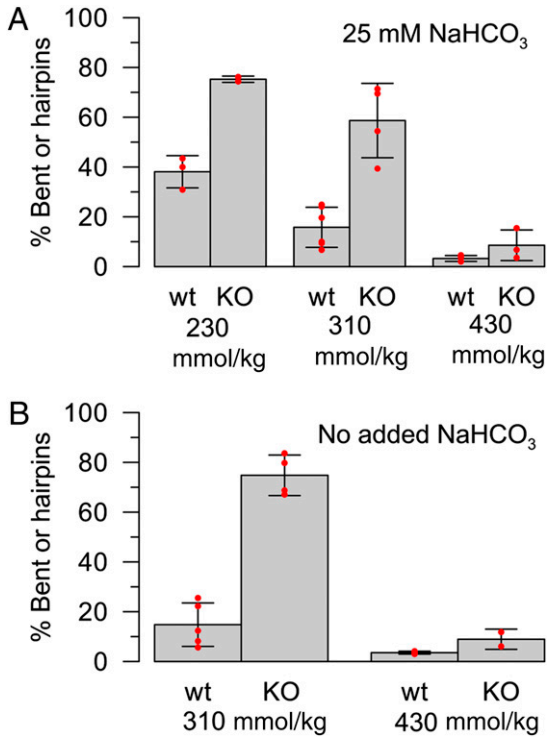

Fig. 5. *Slo3*$^{-/-}$ sperm have osmoregulatory deficits. (*A*) Caudal epididymal sperm were allowed to swim out into a 430 mmol/kg HS medium. At *t* = 0, aliquots were diluted into solutions of different osmolality with added 25 mM $NaHCO_3$. Moving sperm were categorized as either normal or abnormal (bent or hairpin) morphology. The occurrence of abnormal morphology is increased in wt sperm with reductions in osmolality, and this effect is increased in *Slo3*$^{-/-}$ sperm. Each red point represents the estimate from over 100 motile sperm from a single mouse, with error bars indicating SEM. (*B*) Osmolality-related deficits in morphology also occur in the absence of $NaHCO_3$. Each red dot corresponds to the estimate from sperm from a single mouse (*n* = 3–5 for each condition).

(Movies S3 and S4). Thus, in addition to morphological abnormalities, the absence of Slo3 channels had an impact on normal motility in the absence of $NaHCO_3$. This result again suggests that, even before the events leading to alkalization and the elevation of cAMP, the absence of KSper/Slo3 results in functional abnormalities. Thus, for wt sperm released into $NaHCO_3$-free medium, KSper/Slo3 activity at resting cytosolic pH may play some role in the acquisition or maintenance of normal motility.

Discussion

Previous work has demonstrated that an alkalization-activated K^+ current, termed KSper, accounts for most of the K^+ current in CatSper-deficient corpus epididymal sperm (1). The primary candidate for the KSper pore-forming subunit is the pH-dependent Slo3 channel (7), and recently, alkalization-activated K^+ current in testicular sperm was shown to be reduced following *Slo3* KO in another mouse strain (6). Here we show that, in the more mature corpus epididymal sperm, genetic KO of the Slo3 protein produces complete removal of KSper at physiological membrane potentials.

At potentials positive to 0 mV, we observed a second outward current in *Slo3*$^{-/-}$ sperm, termed I_{Kres}. We propose that I_{Kres} represents K^+ efflux through endogenous CatSper channels. Monovalent ion flux through CatSper channels is well-known (11). In addition, both I_{Kres} and CatSper are activated by cytosolic alkalization. The pharmacological information is less clear-cut. Our results require that, for I_{Kres} to be equivalent to CatSper, CatSper must be blocked by both clofilium and quinidine. To our knowledge, neither has been tested on CatSper. Although quinidine/quinine are well-known as general K^+ channel blockers, inhibition of Ca^{2+} channels (20) and nonselective cation channels (21) have also been reported, so inhibition of CatSper might not be surprising. Another unusual aspect of I_{Kres} is its apparent voltage dependence of activation. We considered whether this trait could be consistent with CatSper. CatSper exhibits a weak intrinsic voltage dependence, with activation shifted to negative potentials with alkalization (11). At pH 8.0, CatSper will be strongly activated over most of the voltage range we used. Thus, we hypothesize that the voltage-dependence of I_{Kres} does not reflect intrinsic voltage dependence of activation but, rather, reflects the kinetics of Ca^{2+} unblock and reblock. The activation time constants of I_{Kres} would therefore represent Ca^{2+} dissociation from high-affinity binding sites within the CatSper channels. The observed time constants are generally consistent with expectations for a channel with a micromolar Ca^{2+} binding affinity or lower, a general feature of Ca^{2+}-permeant channels (22). Thus, although a *CatSper*-null, *Slo3*-null mouse would be required to test this point, we propose that I_{Kres} represents K^+ flux through CatSper channels. *Slo3*$^{-/-}$ sperm would therefore provide a useful system for explicit study of CatSper currents.

A remarkable feature of the present results is that, in *Slo3*$^{-/-}$ sperm at potentials negative to 0 mV, there was little detectable K^+ current under the conditions of our experiments, and any residual current can probably be attributed either to ion flux through CatSper channels or from pipette seal resistance. The absence of other conductances seems somewhat surprising given the number of studies that have implicated other kinds of K^+ channels in mouse sperm physiology (23–25). However, no other studies, except for that on KSper, have directly provided identification of putative K^+ currents using direct recordings from corpus epididymal sperm. At least in mouse, it appears that KSper/Slo3 may be critical for two roles: First, it is the sole K^+ conductance available to mediate hyperpolarization during alkalization, and, second, it may also contribute to resting conductances in the absence of sperm activation. Whether this finding will be true in other mammalian species remains to be addressed.

Despite the compelling evidence that Slo3 subunits are the pore-forming elements of KSper channels, previous work has suggested that the KSper is activated at more negative voltages and lower pH than heterologously expressed Slo3 current (Fig. S4). As previously proposed (26), the differences between KSper and Slo3 might arise because of unidentified proteins that coassemble with Slo3 in mouse sperm to generate the native KSper channel. However, we have also identified one other factor that reconciles some of the apparent differences between KSper and Slo3. By using a clofilium-subtraction procedure, we were able to define the intrinsic conductance-voltage (GV) relationship for KSper in native sperm. This finding revealed an apparent blockade of KSper conductance at positive potentials, most likely arising from block by Mg^{2+} and Na^+ in our pipette solutions. As a consequence, the native KSper GV will appear to be less voltage-dependent and somewhat shifted compared with currents in the absence of block, explaining some of the discrepancy in apparent activation properties between KSper and Slo3. However, the almost complete absence of current arising from heterologously expressed Slo3 at pH 7.0 at potentials negative to +100 mV is still inconsistent with the observed activation of KSper at pH 7.0.

The present results confirm the apparent complete infertility of *Slo3*$^{-/-}$ male mice (6). We then considered the underlying basis of the complete infertility of *Slo3*$^{-/-}$ males. One proposal is that KSper-mediated hyperpolarization plays an important role in sustaining Ca^{2+} influx through CatSper channels during cytosolic alkalization (1). It therefore might be expected that reduction of Ca^{2+} influx due to the absence of Slo3 might alter a variety of critical steps in the hyperactivation process, thereby compromising fertility. Another proposal is that a major factor in *Slo3*$^{-/-}$ infertility may arise from a requirement for Slo3 in the acrosome reaction (6). Although we did not address that point, we observed that capacitated *Slo3*$^{-/-}$ sperm retain some reduced ability to fertilize ZP-intact oocytes, suggesting that such sperm can undergo at least part of the normal cascade of events associated with capacitation and formation of the acrosome reaction. Our observation of ~11% fertilization success in ZP-intact oocytes differed from that of Santi et al. (6), who observed ~2% fertilization with either ZP-intact or ZP-free eggs. We also observed a somewhat reduced decrease in CASA-defined progressive motility (wt, 27.2%; *Slo3*$^{-/-}$, 18.5%) in *Slo3*$^{-/-}$ sperm compared with the other report (wt, 31%; *Slo3*$^{-/-}$, 9%). Although we have no explanation for these differences, it is possible that differences in how motile sperm were collected might contribute. However, we believe that any success in an IVF assay indicates that, even in the absence of the Slo3 protein, some sperm can still undergo all of the steps involved in capacitation, penetration of the ZP, and fertilization. Therefore, although *Slo3*$^{-/-}$ sperm undoubtedly exhibit a variety of deficits that will compromise capacitation and fertilization capacity, other factors must be considered as the underlying basis for the complete loss of fertility among breeding pairs.

Our results address two points relevant to the issue of how the absence of KSper/Slo3 may compromise sperm fertility. First, consistent with the observation of an increased frequency of hairpin sperm morphologies in *Slo3*$^{-/-}$ sperm (6), *Slo3*$^{-/-}$ sperm exhibit compromised osmoregulatory capacity. Second, *Slo3*$^{-/-}$ sperm exhibit deficits in ability to acquire normal motility in the absence of $NaHCO_3$, an effect that can be overcome by exposure to 25 mM $NaHCO_3$, consistent with the only modest deficits in progressive motility observed in CASA assays. Based on these observations, we propose that deficits in osmoregulation in *Slo3*$^{-/-}$ sperm result in altered morphology and compromised initial motility, thereby affecting fertilization capacity, independent of any subsequent deficits in capacitation.

For *Slo3*$^{-/-}$ sperm, deficits in osmoregulation and compromised motility in the absence of $NaHCO_3$ suggest that Slo3/KSper plays an important role in sperm function preceding alkalization. Specifically, our results suggest that K^+ efflux

through Slo3/KSper under resting conditions may be essential in minimizing cell swelling following ejaculation and in allowing acquisition of normal motility. It is well established that exposure of caudal spermatozoa to solutions of lowered osmolality results in the occurrence of sperm flagella with angular/bent morphologies (27), and such solutions also produce a pronounced increase in sperm volume (17). Interestingly, quinine also produces a disruption of sperm volume regulation (17) and morphology (27). Together, these considerations point to the idea that a critical role of KSper/Slo3 may be to allow K^+ efflux after dilution into the 310 mmol/kg uterine environment, thereby facilitating regulatory volume decreases. Our results provide no explanation for the differences in motility of *Slo3*$^{-/-}$ sperm in the presence and absence of bicarbonate anion. Bicarbonate elevates cytosolic cAMP through an atypical soluble adenylate cyclase (28–30), modulates depolarization-evoked Ca^{2+} elevations (31), and increases sperm beat frequency (31). Presumably, some cAMP-dependent process might compensate for the absence of Slo3. *Slo3*$^{-/-}$ sperm may therefore be a useful system for evaluating whether mouse sperm express ion channels that are activated during elevation of cAMP.

Materials and Methods

Electrophysiology. Whole-cell recordings of current and voltage behavior used procedures in which cytosolic access was gained through the sperm cytosolic droplet (1, 10, 11). HS was used for sperm swim-out from corpus epididymis for recordings and also as the primary extracellular solution for current-clamp: 135 mM NaCl, 5 mM KCl, 1 mM $MgSO_4$, 2 mM $CaCl_2$, 20 mM Hepes, 5 mM glucose, 10 mM lactic acid, and 1 mM Na·pyruvate at pH 7.4 with NaOH. For most voltage-clamp experiments, cells were bathed in a high-K^+ HS medium: 160 mM KOH, 10 mM Hepes, 150 mM methanesulfonic acid (Mes), and 2 mM $Ca(Mes)_2$, adjusted to pH 7.4 with Mes. A strongly buffered, high-K^+ pipette solution contained 155 mM KOH, 5 mM KCl, 10 mM 1,2-bis(2-aminophenoxy)ethane-*N*,*N*,*N*′,*N*′-tetraacetic acid (BAPTA), 20 mM Hepes, and 115 mM Mes with pH adjusted to 6, 7, or 8 with KOH or Mes. For current clamp recordings in which NH_4Cl was used to alter cytosolic pH, the following pipette solution was used: 144 mM KOH, 5 mM KCl, 5 mM NaCl, 3 mM Mg·ATP, 0.5 mM Na_2·GTP, 1 mM BAPTA, 5 mM Hepes, and 140 mM Mes with pH adjusted to either 6.0 or 8.0 with Mes or KOH.

Solutions were applied directly via a local perfusion system allowing switching between different test solutions. Solution exchange time with this system is typically <1 s. Current waveforms were analyzed either with Clampfit or software developed within this laboratory. All error bars correspond to SEM. All experiments were at room temperature (~22–25 °C). Chemicals were obtained from Sigma.

Analysis of Osmotic Effects on Sperm Morphology and Motility. Caudal epididymes were isolated and gently perforated to allow sperm swim-out into 2 mL of a 430-mosM HS medium (5 mM KCl, 1 mM $MgSO_4$, 2 mM $CaCl_2$, 20 mM Hepes, 5 mM glucose, 10 mM lactic acid, and 1 mM Na·pyruvate, adjusted to pH 7.4 with NaOH), with NaCl adjusted to yield the desired osmolality. After 10 min, epididymal tissues were removed, and 1.5 mL of the solution was placed in a 2-mL microcap for 10 min to allow settling of debris and nonmotile sperm. Then, 250-μL aliquots were diluted into solutions with freshly added $NaHCO_3$, producing the following final solutions: (*i*) 430 mosM HS + 25 mM $NaHCO_3$; (*ii*) 310 mosM HS + 25 mM $NaHCO_3$; (*iii*) 230 mosM HS + 25 mM $NaHCO_3$; and (*iv*) 310 mosM HS with no added $NaHCO_3$. Sperm samples were then pipetted into 20-μ-deep MicroCell chambers (Conception Technologies) for acquisition of videos. Sets of 3.2-s videos were acquired at 80-Hz frame rate, and at least 20 videos were acquired for each condition, allowing ~100 motile sperm to be examined per condition at three different time points. No changes over time were observed in sperm morphology after the initial dilution. From examination of videos, motile sperm were grouped into one of three categories: (*i*) hairpins, (*ii*) bent, or (*iii*) straight. For comparisons of morphology, hairpins and bent were combined into a single category. Only sperm exhibiting movement were considered in these estimates. Video frames were taken at 80 Hz with a Basler A602F high-frame-rate camera using SAVA software (Sisson-Ammons Video Analysis software) on a Nikon Eclipse Ti microscope.

For more details on methods, see *SI Materials and Methods*.

ACKNOWLEDGMENTS. We thank B. Navarro, D. Babcock, and D. Clapham for input during various stages of this work. The Washington University Department of Anesthesiology provided critical support. This work was also supported by National Institutes of Health (NIH) Grants GM066215 and GM081748. Monoclonal antibody anti-mSlo3 N2/16 was obtained from the University of California, Davis/NIH NeuroMab Facility, which is supported by NIH Grant U24NS050606 and maintained by the Department of Neurobiology, Physiology and Behavior, College of Biological Sciences, University of California, Davis. Chengtao Yang provided mSlo3 fusion proteins and Slo3 cDNAs to NeuroMab.

1. Navarro B, Kirichok Y, Clapham DE (2007) KSper, a pH-sensitive K^+ current that controls sperm membrane potential. *Proc Natl Acad Sci USA* 104:7688–7692.
2. Carlson AE, et al. (2003) CatSper1 required for evoked Ca2+ entry and control of flagellar function in sperm. *Proc Natl Acad Sci USA* 100:14864–14868.
3. Visconti PE, Kopf GS (1998) Regulation of protein phosphorylation during sperm capacitation. *Biol Reprod* 59:1–6.
4. Suarez SS (2008) Control of hyperactivation in sperm. *Hum Reprod Update* 14: 647–657.
5. Nixon B, et al. (2010) Elucidation of the signaling pathways that underpin capacitation-associated surface phosphotyrosine expression in mouse spermatozoa. *J Cell Physiol* 224:71–83.
6. Santi CM, et al. (2010) The SLO3 sperm-specific potassium channel plays a vital role in male fertility. *FEBS Lett* 584:1041–1046.
7. Schreiber M, et al. (1998) Slo3, a novel pH-sensitive K^+ channel from mammalian spermatocytes. *J Biol Chem* 273:3509–3516.
8. Zhang X, Zeng X-H, Lingle CJ (2006) Slo3 K^+ channels: Voltage and pH dependence of macroscopic currents. *J Gen Physiol* 128:317–336.
9. Zhang X, Zeng X-H, Xia X-M, Lingle CJ (2006) pH-regulated Slo3 K^+ channels: properties of unitary currents. *J Gen Physiol* 128:301–315.
10. Qi H, et al. (2007) All four CatSper ion channel proteins are required for male fertility and sperm cell hyperactivated motility. *Proc Natl Acad Sci USA* 104:1219–1223.
11. Kirichok Y, Navarro B, Clapham DE (2006) Whole-cell patch-clamp measurements of spermatozoa reveal an alkaline-activated Ca^{2+} channel. *Nature* 439:737–740.
12. Tang QY, Zhang Z, Xia XM, Lingle CJ (2010) Block of mouse Slo1 and Slo3 K+ channels by CTX, IbTX, TEA, 4-AP and quinidine. *Channels (Austin)* 4:22–41.
13. Fedida D (1997) Gating charge and ionic currents associated with quinidine block of human Kv1.5 delayed rectifier channels. *J Physiol* 499:661–675.
14. Tseng GN, Zhu B, Ling S, Yao JA (1996) Quinidine enhances and suppresses Kv1.2 from outside and inside the cell, respectively. *J Pharmacol Exp Ther* 279:844–855.
15. Doi T, et al. (1995) Subunit-specific inhibition of inward-rectifier K^+ channels by quinidine. *FEBS Lett* 375:193–196.
16. Yeung CH, Barfield JP, Cooper TG (2006) Physiological volume regulation by spermatozoa. *Mol Cell Endocrinol* 250:98–105.
17. Yeung CH, Anapolski M, Cooper TG (2002) Measurement of volume changes in mouse spermatozoa using an electronic sizing analyzer and a flow cytometer: Validation and application to an infertile mouse model. *J Androl* 23:522–528.
18. Chen Q, et al. (December 7,2010) Aquaporin3 is a sperm water channel essential for postcopulatory sperm osmoadaptation and migration. *Cell Res*, 10.1038/cr.2010.169.
19. Kawai Y, Hata T, Suzuki O, Matsuda J (2006) The relationship between sperm morphology and in vitro fertilization ability in mice. *J Reprod Dev* 52:561–568.
20. Solntseva EI (1987) *Neirofiziologiia* 19:413–417.
21. Gray MA, Argent BE (1990) Non-selective cation channel on pancreatic duct cells. *Biochim Biophys Acta* 1029:33–42.
22. Almers W, McCleskey EW, Palade PT (1984) A non-selective cation conductance in frog muscle membrane blocked by micromolar external calcium ions. *J Physiol* 353: 565–583.
23. Barfield JP, Yeung CH, Cooper TG (2005) Characterization of potassium channels involved in volume regulation of human spermatozoa. *Mol Hum Reprod* 11:891–897.
24. Darszon A, et al. (2007) Ion channels in sperm motility and capacitation. *Soc Reprod Fertil Suppl* 65:229–244.
25. Navarro B, Kirichok Y, Chung JJ, Clapham DE (2008) Ion channels that control fertility in mammalian spermatozoa. *Int J Dev Biol* 52:607–613.
26. Yang CT, Zeng XH, Xia XM, Lingle CJ (2009) Interactions between beta subunits of the KCNMB family and Slo3: Beta4 selectively modulates Slo3 expression and function. *PLoS ONE* 4:e6135.
27. Yeung CH, Sonnenberg-Riethmacher E, Cooper TG (1999) Infertile spermatozoa of c-ros tyrosine kinase receptor knockout mice show flagellar angulation and maturational defects in cell volume regulatory mechanisms. *Biol Reprod* 61:1062–1069.
28. Buck J, Sinclair ML, Schapal L, Cann MJ, Levin LR (1999) Cytosolic adenylyl cyclase defines a unique signaling molecule in mammals. *Proc Natl Acad Sci USA* 96:79–84.
29. Chen Y, et al. (2000) Soluble adenylyl cyclase as an evolutionarily conserved bicarbonate sensor. *Science* 289:625–628.
30. Jaiswal BS, Conti M (2001) Identification and functional analysis of splice variants of the germ cell soluble adenylyl cyclase. *J Biol Chem* 276:31698–31708.
31. Wennemuth G, Carlson AE, Harper AJ, Babcock DF (2003) Bicarbonate actions on flagellar and Ca^{2+} -channel responses: Initial events in sperm activation. *Development* 130:1317–1326.